A preliminary approach to the MSFR control issues

Claudia Guerrieri, Antonio Cammi, Lelio Luzzi *

Politecnico di Milano – Department of Energy, CeSNEF (Enrico Fermi Center for Nuclear Studies), via Ponzio 34/3, 20133 Milano, Italy

Received 3 January 2013
Accepted 5 August 2013
Available online 5 September 2013

1. Introduction

The Molten Salt Reactor (MSR) is one of the six systems selected in the frame of the Generation IV International Forum to be deployed in the medium/long term for a proliferation resistant, safe, economic competitive and sustainable nuclear energy production (GIF-IV, 2002). After the first studies carried out at the Oak Ridge National Laboratory (ORNL) during the sixties in the frame of the Molten Salt Reactor Program, the interest in this technology faded out (MacPherson, 1985). It met a true revival only recently, thanks to the Gen-IV Initiative. Originally, MSRs were proposed as thermal-neutron spectrum graphite-moderated concepts. Recently, the interest has been focused on fast-spectrum reactors. As a matter of fact, the Molten Salt Fast Reactor (MSFR), designed in the frame of the EVOL Project of the EURATOM 7th Framework Programme (EVOL, 2012), has been recognised as a promising alternative to fast-neutron systems adopting solid fuel and has been adopted as Generation IV MSR reference configuration (GIF-IV, 2009).

For the MSFR, no control-oriented analyses have been carried out, yet. Actually, the good dynamic behaviour and load-following properties of the MSFR (and MSRs in general) (Guerrieri et al., 2013) and the early stage of the plant design, combined with some pressing issues regarding for example materials and chemistry of the salt, overshadowed the issues concerning plant control. In this work, some preliminary considerations are drawn on the evaluation of the degree of interaction between manipulated (input) and controlled (output) variables, paving the way for the definition of a control strategy. Herein, an objective criterion is proposed for the input/output pairing, based on analyses used in the field of the linear system theory and Multiple-Input Multiple-Output (MIMO) system control (Skogestad and Postlethwaite, 2001).

The paper is organised as follows: Section 2 provides a basic description of the analysed system as well as a detailed explanation of the developed model and of the main assumptions and simplifications adopted. In Section 3, the degree of interaction between input and output variables of the modelled system is investigated and an objective criterion is proposed for input/output pairing. In Section 4, some control schemes are implemented, analysing the transient response of the closed loop system. Finally, the main conclusions are outlined in Section 5.

2. MSFR description and modelling

The case study adopted in this work is the recently-proposed MSFR. A schematic view of the reactor primary circuit is reported in Fig. 1 (Brovchenko et al., 2012). The MSFR is a 3 GW_{th} reactor fuelled with an initial mixture of fissile isotopes and fertile thorium in the form of UF_4 and ThF_4 dissolved in a fluoride salt of LiF with a proportion of 22.5 mol%. The reactor core is a cylinder whose diameter is equal to the height, filled completely with liquid fuel. No solid moderator is present inside the core, and no structural

* Corresponding author. Tel.: +39 02 2399 6326.
E-mail address: lelio.luzzi@polimi.it (L. Luzzi).

Nomenclature

c_j	delayed neutron precursor concentration – jth precursor group (m^{-1})
C_j	delayed neutron precursor population – jth precursor group (–)
c_p	specific heat ($J\,kg^{-1}\,K^{-1}$)
f_i	constant related to the fraction of decay heat isotopes per fission (–)
F_i	population of the ith group of decay heat isotopes (–)
G	gain matrix
h	heat transfer coefficient ($W\,m^{-2}\,K^{-1}$)
H	height (m)
I	input (–)
K_D	Doppler constant (–)
M	mass (kg)
n	neutron concentration (m^{-1})
N	neutron population (–)
O	output (–)
P	power (W)
q'	power source ($W\,m^{-1}$)
s	Laplace variable ($rad\,s^{-1}$)
t	time (s)
T	temperature (K)
T^*	average temperature (K)
U	overall heat transfer coefficient between primary and intermediate salt ($W\,K^{-1}$)
x	axial coordinate (m)

Greek symbols

α_{ex}	density feedback coefficient of the fuel (K^{-1})
β	total fraction of delayed neutrons (–)
β_j	fraction of delayed neutron precursors for the jth precursor group (–)
Γ	mass flow rate ($kg\,s^{-1}$)
Λ	mean neutron generation time (s)
λ_j	decay constant of the jth precursor group (s^{-1})
λ_i	decay constant of the ith group of decay heat isotopes (s^{-1})
λ_{ij}	RGA element on row i and column j
ρ	reactivity (–)
ρ_{cr}	reactivity provided by the control rods (–)
ρ_t	reactivity due to temperature feedback (–)
τ_c	core transit time (s)
τ_e	external (out-of-core) transit time (s)
ω	angular frequency ($rad\,s^{-1}$)
δ and Δ	variations

Superscripts and subscripts

0	steady state
1	primary circuit
2	intermediate circuit
av	average
c	core
cool	coolant salt
f	fuel salt
h	heat exchanger
in	inlet
out	outlet
ref	reference

elements as well. The core is radially surrounded by a fertile blanket to allow breeding. Around the blanket a wall made of B_4C is proposed to protect the heat exchangers and the other structures from the neutron flux. Axial reflectors are present over and below the core to improve neutron economy. Under the lower reflector a draining system is designed to allow the evacuation of the fuel from the core for safety purposes. During operation, the liquid fuel, heated up to an average temperature of 700 °C, flows upward in the core until it reaches the salt collectors in the upper plenum. Before being re-injected into the core, the salt flows towards a system of sixteen heat exchangers that extract the thermal power produced inside the core and transfer it to an intermediate circuit working with molten FLiNaK. A detailed overview of the MSFR primary circuit can be found in (Brovchenko et al., 2012). As concerns the primary heat exchangers, their design has not been finalised yet. For the purpose of this work, a preliminary design of a shell and tube heat exchanger[1] has been considered to allow the modelling of the entire primary circuit. The data used for the MSFR modelling, as well as the parameters of the heat exchanger adopted in this work, are shown in Table 1. The neutronics constants have been computed according to the methodology adopted in (Fiorina et al., 2012), which focused on the analysis of MSFR core physics in terms of safety parameters, core reactivity, neutron spectra and flux spatial distribution, mainly using the deterministic code ERANOS 2.2N (Rimpault et al., 2002).

[1] For the purpose of this analysis, a shell and tube heat exchanger has been considered coherently with the experience carried out at the Oak Ridge National Laboratory. Nonetheless, other heat exchanger configurations are currently being evaluated in the frame of the EVOL Project.

For the purpose of the analysis carried out in this work, a simple model of the primary circuit has been set-up, based on point-kinetics description of neutronics and one-dimensional description of delayed neutron precursors (DNP) and energy transport.

As far as the neutron and DNP populations are concerned, the governing equations are the following:

$$\frac{dN(t)}{dt} = \frac{\rho(t) - \beta}{\Lambda} N(t) + \sum_{j=1}^{8} \lambda_j C_j(t), \tag{1}$$

$$\frac{\partial c_j(x,t)}{\partial t} - \frac{\Gamma_1 H^c}{M_f^c} \frac{\partial c_j(x,t)}{\partial x} = \frac{\beta_j}{\Lambda} n(x,t) - \lambda_j c_j(x,t) \quad for\, j = 1, \ldots 8. \tag{2}$$

where C_j and N are the integral over the core height of the spatial dependent variables $c_j(x,t)$ and $n(x,t)$, the last one obtained assuming the neutron population distributed according to a cosine function (see the Nomenclature section for the complete list of the adopted symbols). To complete the DNP model, a boundary condition is imposed between the inlet and the outlet of the reactor core, as follows:

$$c_j(0,t) = c_j(H^c, t - \tau_e) e^{-(\lambda_j/\tau_e)} \quad for\, j = 1, \ldots 8. \tag{3}$$

The drift of the delayed neutron precursors acts reducing the fraction of delayed neutrons available to sustain the fission reaction and consequently the margin of the system towards the condition of prompt-criticality, which is important as concerns the reactor control. Depending on the flow pattern within the core the approximation related to the evaluation of the fraction of delayed neutrons in circulating fuel condition through a one-dimensional approach

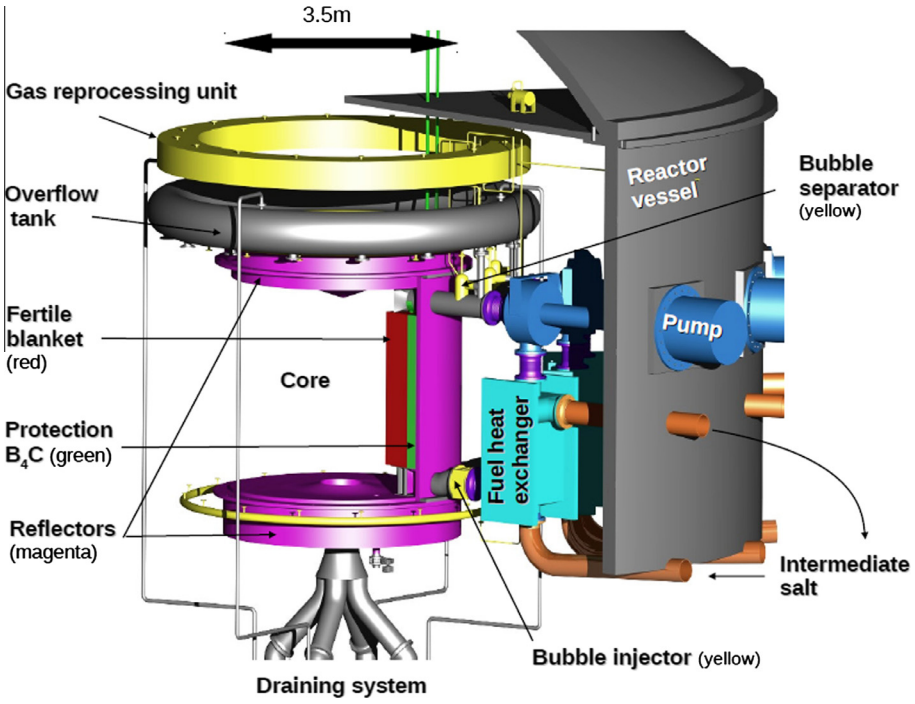

Fig. 1. View of the MSFR primary circuit (Brovchenko et al., 2012).

can be more or less significant. However, the set-up of more detailed modelling approaches is out of the aim of the present analysis.

The reactivity term in Eq. (1) is the sum of three contributions, namely: the reactivity provided by the control rods[2], used also as input for the system; the reactivity feedback due to temperature variations; and the reactivity contribution provided to guarantee steady-state, that compensates the loss of reactivity with respect to static-fuel condition due to the decay of DNPs in the out-of-core part of the primary circuit. It is worth pointing out that a system of operational control rods has not been included in the design of the reactor. Nonetheless, such system will be modelled here for the sake of a general investigation of the system behaviour.

The model includes also the description of the decay heat generated by the isotopes present in the system. These isotopes have been gathered in the three groups, each one responsible of a portion of decay power released with a specific time constants. A fully lumped description has been adopted.

$$\frac{dF_i(t)}{dt} = f_i\lambda_i N(t) - \lambda_i F_i(t) - \frac{1}{\tau_c}F_i(t) + \frac{1}{\tau_c}F_i(t-\tau_e)e^{-(\lambda_i\tau_e)} \quad \text{for } i = 1,\dots 3. \tag{4}$$

The coefficients f_i and λ_i used in the model have been obtained by interpolation of the curves of decay heat after the reactor shutdown computed by means of the Monte Carlo neutron transport code SERPENT (Guerrieri et al., 2012).

The energy balance in the core has been described using a one-dimensional approach, according to Eq. (5). Heat exchange between the fuel and the salt in the blanket has been neglected considering adiabatic walls.

$$\frac{\partial T_f(x,t)}{\partial t} - \frac{\Gamma_1 H^c}{M_f^c}\frac{T_f(x,t)}{\partial x} = \frac{H^c}{M_f^c c_{p_f}} q'(x,t). \tag{5}$$

[2] Actually, this contribution could be related to other sources of reactivity (e.g., addition/removal of burnable poisons into the fuel).

It should be mentioned that the MSFR is characterised by a potentially complex flow pattern considering the current core design, although different solutions are presently being considered to optimise the flow pattern reducing the areas of salt recirculation (e.g., hourglass shaping of the core, distribution plate located at the core inlet, etc.). Nevertheless, the one-dimensional thermal–hydraulic model was preferred to more detailed modelling approaches because it allows a straightforward simulation of the system dynamics with low computational requirements, which is usually preferable when dealing with control-oriented analyses.

A one-dimensional approach has been used also to describe the energy balance at the two sides of the heat exchanger:

$$\frac{\partial T_f(x,t)}{\partial t} - \frac{\Gamma_1 H^h}{M_f^h}\frac{\partial T_f(x,t)}{\partial x} = \frac{H^h}{M_f^h c_{p_f}} q'(x,t) + \frac{U}{M_f^h c_{p_f}}[T_{cool}(x,t) - T_f(x,t)], \tag{6}$$

$$\frac{\partial T_{cool}(x,t)}{\partial t} - \frac{\Gamma_2 H^h}{M_{cool}^h}\frac{\partial T_{cool}(x,t)}{\partial x} = -\frac{U}{M_{cool}^h c_{p_{cool}}}[T_{cool}(x,t) - T_f(x,t)]. \tag{7}$$

The source term in Eq. (6) allows for the fraction of decay power that is released with some delay in the out-of-core part of the primary circuit. A uniform distribution of the decay heat is considered both inside the core and in the heat exchanger. Also, it is supposed that no power is released in the hot and cold legs. Since both the primary and the intermediate salt flow rates are adopted as manipulated variables, the dependence of the heat transfer coefficients at the two sides of the heat exchanger on the salt velocity has been included in the model through an expression like Eq. (8), where the coefficient of the power has been set according to the Dittus–Boelter correlation (Dittus and Boelter, 1930).

$$h = h_0\left(\frac{\Gamma}{\Gamma_0}\right)^{0.8}. \tag{8}$$

Table 1
MSFR data adopted in the analysis (Merle-Lucotte et al., 2011; Fiorina et al., 2012).

Nominal thermal power (MW_{th})	3000
Core inlet/outlet temperatures (K)	923/1023
Core height (m)	2.255
Mass of salt in the core (kg)	37,124
Mass of salt out of core (primary circuit) (kg)	37,124
Mass of salt in the heat exchangers (kg)	12,993
Specific heat of the fuel salt ($J\,kg^{-1}\,K^{-1}$)	1594
Fuel salt mass flow rate ($kg\,s^{-1}$)	18,964
Primary circuit transit time (s)	3.9
Core transit time (s)	1.95
Hot leg transit time (s)	0.6
Cold leg transit time (s)	0.6
Height of the heat exchangers (m)	2
Overall heat transfer coefficient between the primary and the intermediate salt ($W\,K^{-1}$)	2.165×10^7
Heat transfer coefficient fuel salt side ($W\,m^{-2}\,K^{-1}$)	11,333
Heat transfer coefficient coolant salt side ($W\,m^{-2}\,K^{-1}$)	13,355
Heat transfer area in the heat exchangers (m^2)	3240
Mass of coolant salt in the heat exchangers (kg)	13,365
Specific heat of the coolant salt ($J\,kg^{-1}\,K^{-1}$)	1861
Coolant salt mass flow rate ($kg\,s^{-1}$)	27,018
Mean neutron generation time Λ (μs)	0.963
Doppler constant (pcm)	3161.39
Density feedback coefficient of the fuel ($pcm\,K^{-1}$)	−2.45
Fraction of DNPs (1st group of precursors) (–)	23.74×10^{-5}
Fraction of DNPs (2nd group of precursors) (–)	47.25×10^{-5}
Fraction of DNPs (3rd group of precursors) (–)	41.32×10^{-5}
Fraction of DNPs (4th group of precursors) (–)	63.94×10^{-5}
Fraction of DNPs (5th group of precursors) (–)	100.55×10^{-5}
Fraction of DNPs (6th group of precursors) (–)	15.22×10^{-5}
Fraction of DNPs (7th group of precursors) (–)	21.44×10^{-5}
Fraction of DNPs (8th group of precursors) (–)	4.60×10^{-5}
Total fraction of DNPs (–)	318.06×10^{-5}
DNP decay constant (1st group of precursors) (s^{-1})	1.25×10^{-2}
DNP decay constant (2nd group of precursors) (s^{-1})	2.83×10^{-2}
DNP decay constant (3rd group of precursors) (s^{-1})	4.25×10^{-2}
DNP decay constant (4th group of precursors) (s^{-1})	1.33×10^{-1}
DNP decay constant (5th group of precursors) (s^{-1})	2.93×10^{-1}
DNP decay constant (6th group of precursors) (s^{-1})	6.67×10^{-1}
DNP decay constant (7th group of precursors) (s^{-1})	1.64
DNP decay constant (8th group of precursors) (s^{-1})	3.56
Power fraction associated to the 1st group of decay heat (–)	0.0117
Power fraction associated to the 2nd group of decay heat (–)	0.0129
Power fraction associated to the 3rd group of decay heat (–)	0.0186
Decay constant (1st group of decay heat) (s^{-1})	0.1974
Decay constant (2nd group of decay heat) (s^{-1})	0.0168
Decay constant (3rd group of decay heat) (s^{-1})	3.58×10^{-4}

Finally, the temperature reactivity feedback has been modelled by dividing the Doppler effect and that one related to the density variation within the fuel into two separate contributions, which are function of an average temperature computed considering the neutron flux shaped according to a cosine.

$$\Delta\rho_t(t) = -K_D \ln\left(\frac{T_f^*(t)}{T_{f0}^*}\right) + \alpha_{ex}(T_f^*(t) - T_{f0}^*). \quad (9)$$

This formulation is based on preliminary studies carried out by Fiorina et al. (2012), who has shown that the dependence of the reactivity coefficient related to the Doppler effect at a generic temperature T is of the form $d\rho/dT = -K_D/T$, similarly to what occurs in oxide-fuelled fast reactors (Waltar et al., 2012).

All the spatial-dependent equations have been discretized considering twenty axial regions in the core and at the two sides of the heat exchanger, and have been implemented in Simulink (2012).

The system herein analysed is a MIMO system. In particular, four inputs and four outputs have been selected. The outputs are the thermal power, the inlet and the outlet core temperatures, and the temperature of the coolant salt at the outlet of the heat exchanger. The inputs are the reactivity provided by the control rods, the primary and the intermediate salt flow rates, and the inlet salt temperature at the secondary side of the heat exchanger. With reference to the whole plant, the inlet salt temperature at the secondary side of the heat exchanger should be considered an output rather than an input. However, in this work, it has been included among the input variables in order to allow the evaluation of the dynamic behaviour of the system in response to a variation of the salt temperature in the cold leg of the intermediate circuit that can occur as a consequence of a control action on the secondary circuit (that is not included in the model).

For the purpose of the Relative Gain Array (RGA) analysis carried out in this work, the model has been linearised through a dedicated linearisation tool of Simulink. All the equations that govern the system behaviour have been expressed in terms of deviation variables, defined as the difference between the variable itself and its steady-state value. Finally, a scaling of the system has been performed, dividing the input and output variables by suitable scaling factors, as usual in the control analysis of MIMO systems (Skogestad and Postlethwaite, 2001). These scaling factors have been chosen according to an approximate evaluation of the expected range of variation of each variable in operative conditions. In particular, the nominal values have been adopted for scaling the thermal power and the flow rates in the primary and intermediate circuits, a reference value of 50 °C has been adopted for all the temperatures (approximately equal to the margin with respect to the solidification point for both the fuel and the coolant salt), and the fraction of delayed neutrons for static fuel has been considered for scaling the control rod provided-reactivity. These scaled quantities are referred to as normalised variables in the following.

3. Relative Gain Array analysis

Useful information about the most favourable pairings between input and output variables of a MIMO system for decentralized control can be obtained from the analysis of the RGA, which was originally introduced as a steady-state measure of the interactions that occur in a square system (Bristol, 1966). Here, some basic features of the RGA are briefly introduced for convenience, further details can be found for example in (Skogestad and Postlethwaite, 2001). Consider a stable linear system at steady state. If a change of one input occurs, the system evolves towards a new equilibrium characterised by different values of the outputs. The open loop gain of a general input u_j with respect to the output y_i is defined as: $g_{ij} = \Delta y_i/\Delta u_j$. Suppose now that, for the same variation of u_j, the other inputs can be varied in such a way that all the outputs except y_i return to their original value at the end of the transient. Generally, the variation of y_i (indicated as Δy_{i_cl} in this case) will be different from Δy_i. The closed loop gain of the input u_j with respect to the output y_i is defined as $h_{ij} = \Delta y_{i\_cl}/\Delta u_j$. A representation of the two described situations is shown in Fig. 2.

The importance of the RGA is that each element of this matrix is equal to the ratio between the open loop and closed loop gains between the input u_j and the output y_i. The RGA of a square system can be computed by $RGA = G(0)x(G(0)^{-1})^T$, where $G(0)$ is the matrix of the static gains and the symbol x denotes the Hadamard product (or Schur product). A set of rules are adopted that help in choosing the most convenient pairings between inputs and outputs (Skogestad and Postlethwaite, 2001), namely: (1) avoid choosing pairs with corresponding RGA elements negative (because this causes a gain reversal by closing the other loops); and (2) choose pairing with corresponding RGA elements close to 1. An RGA element equal to 1 suggests that the input variable can be used to control the corresponding output variable with no interactions from the other control loops of the system. For this reason, input/output pairings corresponding to low RGA elements or RGA elements notably higher than 1 should be avoided. The original RGA

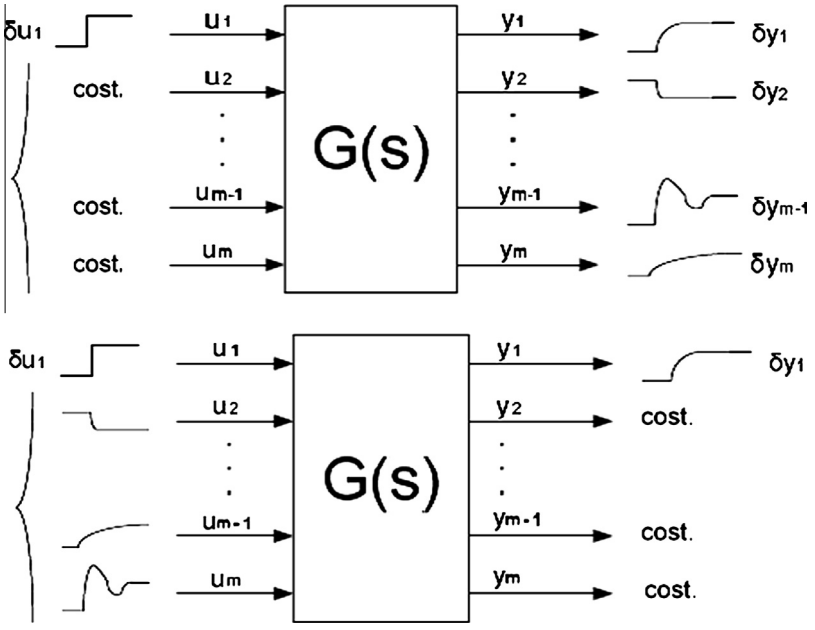

Fig. 2. Scheme of the open loop and closed loop gains of a MIMO system: output y_1 with respect to input u_1.

definition was generalised to consider also frequencies different from zero and non-square systems. For the first case, the RGA matrix corresponding to an angular frequency ω can be computed as $RGA_\omega = G(\omega) x (G(\omega)^{-1})^T$, where $G(\omega)$ is the matrix of the gains of the system at that particular angular frequency. Based on this definition, an improvement of the second pairing rule is to choose pairs corresponding to RGA elements close to 1 at a frequency corresponding to the closed loop time constant (Skogestad and Postlethwaite, 2001). The extension of the RGA for non-square systems was first suggested by Chang and Yu (1990), by the use of the Moore–Penrose pseudo-inverse of the static gain matrix $G(0)$ (i.e., $G(0)^\dagger$) in the expression of the RGA. The resulting matrix is referred to as Non-square Relative Gain Array (NRGA), and represents a simple and effective screening tool for selecting inputs and outputs of a non-square system (Chang and Yu, 1990; Cao and Rossiter, 1997). When the inputs exceed the number of controlled outputs, the selection rule proposed in literature is to avoid using those ones corresponding to columns where the sum of the elements is much smaller than 1. On the contrary, when the controlled outputs exceed the number of inputs, one should avoid using outputs corresponding to rows where the sum is much smaller than 1. At any rate, the aim of this selection is to obtain a square system that can be analysed using the classical formulation of the RGA.

In this section, the RGA (and NRGA) analysis has been applied to the study of the degree of coupling of input and output variables of the modelled MSFR system. This analysis gives useful information in view of the preliminary definition of a possible control scheme and allows an assessment of the most favourable pairing options for decentralised control. Since there are no indications either on the control strategy to adopt for the MSFR or on the output variables that must be controlled, different scenarios have been investigated in this work. Moreover, we have considered the control action to occur in the range of low frequencies, as usual in the regulation of nuclear reactors, adopting an angular frequency of 0.1 rad s^{-1} as approximate upper limit for the bandwidth of the closed loop system (Hetrick, 1993). In the following, the results of the analysis will be referred to this frequency range.

Since we are dealing with a square system (featuring four inputs and four outputs), in principle all the output variables can be controlled. The RGA of the system for this first case (referred to as case i in the following) is shown in Table 2, where each element of the table is the ratio between g_{ij} and h_{ij} (the output variables being indicated on the rows, and the input variables on the columns). When all the inputs are used as manipulated variables for the control of the system outputs, the RGA analysis suggests to pair the power with the fuel salt flow rate, the core outlet temperature with the control rod-provided reactivity, the core inlet temperature with the coolant flow rate, and the temperature of the coolant at the outlet of the heat exchanger with that one at its inlet. In this case, the pairing of the power with the fuel flow rate is penalised compared with the other control loops since the corresponding RGA element is smaller than 0.5.

Other scenarios have been investigated, featured by different choices regarding the scheme of control. In particular, different subsets of controlled variables have been considered, assuming that we are not interested in the control of all the outputs of the system. Table 3 shows the NRGA in case the controlled variables are only the power, the inlet (case ii-A) or the outlet (case ii-B) core temperature and the coolant temperature at the outlet of the heat exchanger. Since there are only three controlled variables in this case, a selection criterion is used. The smaller column sum of the NRGA for the temperature of the intermediate salt at the inlet of the heat exchanger (both for case ii-A and ii-B) suggests that the reactivity and the two flow rates should be adopted as control variables. The reduced systems have been analysed using the RGA. The resulting input/output pairing is highlighted for convenience in the second section of Table 3.

Table 2
Case i: RGA for the system with four controlled variables, namely: power, core outlet temperature, core inlet temperature, temperature of the coolant at the outlet of the heat exchanger.

Case i				
	ρ_{cr}	Γ_1	Γ_2	$T_{cool}^{h\ in}$
P	0.01	**0.38**	1.02	−0.41
$T_f^{c\ out}$	**0.63**	0.31	0.20	−0.14
$T_f^{c\ in}$	0.36	0.30	**1.16**	−0.82
$T_{cool}^{h\ out}$	0.00	0.00	−1.37	**2.37**

Bold values highlight the elements in the RGA matrices that correspond to the chosen input/output pairs.

Table 3
Case ii-A: NRGA and RGA for the system with three controlled variables, namely: power, core outlet temperature and temperature of the coolant at the outlet of the heat exchanger. Case ii-B: NRGA and RGA for the system with three controlled variables, namely: power, core inlet temperature and temperature of the coolant at the outlet of the heat exchanger.

Case ii-A					Case ii-B				
	ρ_{cr}	Γ_1	Γ_2	$T_{cool}^{h\ in}$		ρ_{cr}	Γ_1	Γ_2	$T_{cool}^{h\ in}$
P	0.09	0.51	0.32	0.08	P	−0.19	0.69	0.67	−0.17
$T_f^{c\ out}$	0.75	0.25	0.00	0.00	$T_f^{c\ in}$	1.52	−0.65	0.43	−0.31
$T_{cool}^{h\ out}$	0.15	0.23	0.30	0.33	$T_{cool}^{h\ out}$	−0.47	0.70	−0.34	1.11
$\Sigma_{columns}$	0.99	0.98	0.61	0.41	$\Sigma_{columns}$	0.86	0.74	0.76	0.64
P	0.08	**0.48**	0.44		P	−0.33	0.89	**0.44**	
$T_f^{c\ out}$	**0.75**	0.25	0.00		$T_f^{c\ in}$	**2.21**	−1.21	0.00	
$T_{cool}^{h\ out}$	0.17	0.26	**0.56**		$T_{cool}^{h\ out}$	−0.89	**1.32**	0.56	

Bold values highlight the elements in the RGA matrices that correspond to the chosen input/output pairs.

In case ii-A, the pairing for the power and for the core outlet temperature suggested by the RGA analysis is the same as in the previous analysed case (case i). On the other hand, if the power, the core inlet temperature and the temperature of the coolant at the outlet of the heat exchanger are the controlled variables (case ii-B), the RGA suggests to pair the first with the coolant flow rate in the intermediate circuit, the second with the control rod-provided reactivity and the third with the fuel flow rate.

A similar analysis has been carried out assuming that the variables to control are only the power and one temperature in the core. The results are indicated in Table 4. Also in this case a screening criterion must be applied, since the number of inputs exceeds the number of controlled variables. When the core outlet temperature needs to be controlled together with the power (case iii-A), the screening criterion based on the analysis of the sum of the elements of the NRGA matrix suggests to exclude the coolant flow rate and the coolant temperature at the inlet of the heat exchanger from the set of manipulated inputs. On the contrary, when the core inlet temperature needs to be controlled (case iii-B), the fuel salt flow rate is one of the two dischargeable inputs together with the coolant temperature at the inlet of the heat exchanger.

In Fig. 3, the modules of the RGA elements referring to the selected pairings for cases i, ii-A, ii-B, iii-A and iii-B are plotted as a function of the frequency. The variation of the RGA elements between steady-state and angular frequencies up to 0.1 rad s^{-1} are small, confirming the pairing choices made above.

In brief, the following general indications have been obtained. The system is characterised by a very favourable interaction between the reactivity and the temperature in the core (particularly with the core outlet temperature). Therefore, when possible, this pairing should be chosen. The power should be controlled either by the fuel salt flow rate or by the coolant flow rate in the intermediate circuit. In particular, when the inlet core temperature needs to be controlled, the power should be paired with the intermediate salt flow rate, otherwise the pairing with the primary salt flow rate should be preferred. The temperature of the intermediate salt at the outlet of the heat exchanger can be controlled by the flow rate in the primary circuit or by the coolant flow rate in the intermediate circuit. When these two last variables are used for the control of other quantities, the temperature at the inlet of the heat exchanger can be adopted.

In this section, the RGA analysis has been carried out supposing that all the inputs can be adopted as manipulated variables. In the sequel, starting from defined sets of input variables, some control schemes are analysed and implemented, showing the time dependent response of the closed loop system.

Table 4
Case iii-A: NRGA and RGA for the system with two controlled variables, namely: power and core outlet temperature. Case iii-B: NRGA and RGA for the system with two controlled variables, namely: power and core inlet temperature.

Case iii-A					Case iii-B				
	ρ_{cr}	Γ_1	Γ_2	$T_{cool}^{h\ in}$		ρ_{cr}	Γ_1	Γ_2	$T_{cool}^{h\ in}$
P	0.04	0.43	0.39	0.13	P	0.12	0.22	0.49	0.16
$T_f^{c\ out}$	0.78	0.23	−0.01	0.00	$T_f^{c\ in}$	0.54	0.16	0.23	0.08
$\Sigma_{columns}$	0.83	0.67	0.38	0.13	$\Sigma_{columns}$	0.66	0.38	0.72	0.24
	ρ_{cr}	Γ_1				ρ_{cr}	Γ_2		
P	0.25	**0.75**			P	0.27	**0.73**		
$T_f^{c\ out}$	**0.75**	0.25			$T_f^{c\ in}$	**0.73**	0.27		

Bold values highlight the elements in the RGA matrices that correspond to the chosen input/output pairs.

4. Analysis of possible schemes for the control of the power and the temperature in the core

In this section, some control schemes for the modelled MSFR system have been investigated. Herein, the attention is focused on the control of only two outputs (i.e., the thermal power and one temperature in the core) assuming different sets of control variables. Like in the previous section, the RGA analysis has been applied to choose the most convenient input/output pairing. The control schemes suggested by the RGA analysis have been implemented using conventional Proportional–Integral (PI) controllers (a schematic representation of the adopted feedback control is shown in Fig. 4). This analysis allowed the preliminary assessment of the proposed schemes of control through the evaluation of the transient response of the closed loop system, as well as a comparison of different control strategies.

4.1. Reactivity and flow rate in the intermediate circuit as control variables

In this subsection, it is supposed that only the control rod-provided reactivity and the coolant flow rate are used as control variables to regulate the system. Two options have been considered: the first is featured by the use of the thermal power and the core outlet temperature as controlled variables (case 1-A), whereas in the second case the controlled variables are the thermal power and the core inlet temperature (case 1-B). Table 5 shows the RGA corresponding to the case in which the control rod-provided reactivity and the salt flow rate in the intermediate circuit are used as control variables to regulate the thermal power and the core outlet temperature. If the controlled variables are the thermal power and the core inlet temperature, the RGA of the system is the same shown in Table 4 (case iii-B).

In the case 1-A, the RGA matrix of the system has small negative diagonal elements and therefore the corresponding pairing (control of the power by means of the control rod-provided reactivity and of the core outlet temperature by means of the coolant flow

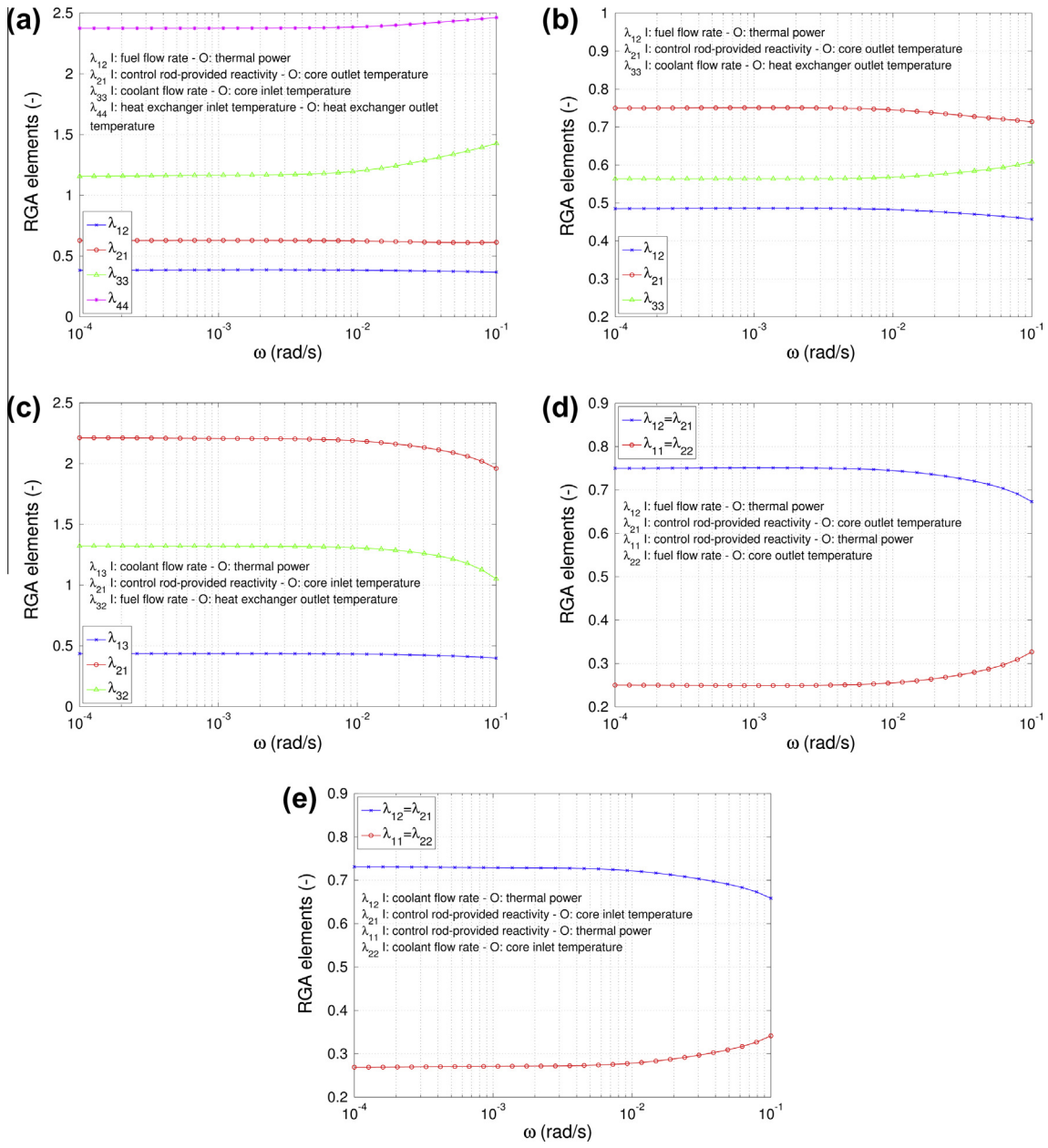

Fig. 3. Variation of the RGA elements of Tables 2–4 corresponding to the selected pairings (i.e., λ_{ij} is the element in the matrix on the row i and column j), between steady-state and an angular frequency of 0.1 rad s^{-1}: (a) case i; (b) case ii-A; (c) case ii-B; (d) case iii-A; (e) case iii-B.

rate) must be avoided. As mentioned, negative elements in the RGA matrix suggest a gain reversal between input (I)/output (O) variables by closing the other loops. Thus, the pairing of variables corresponding to negative elements in the RGA can cause the occurrence of instability when one loop becomes inactive, for example because of saturation. In this case, the presence of negative elements on the diagonal of the RGA can be explained as follows. Considering the open loop response of the system, an increase of the coolant flow rate causes an increase of the overall heat transfer coefficient between the primary and the intermediate circuit. The core average temperature decreases and the temperature feedback acts increasing the power. Following the power increase, the average temperature in the core starts to rise again. The transient ends when the average temperature of the core returns to its initial value. In the meanwhile, the core outlet temperature rises until the system reaches the new steady state. If the coolant flow rate is increased while keeping fixed the power with an action on the reactivity provided by the control rods, the core outlet temperature decreases, instead. This explains how the open loop gain between the intermediate salt flow rate and the core outlet temperature, which is originally positive, becomes negative due to the interaction between the two control loops. For this reason, in the case 1-A, the only feasible choice is to couple the power with the intermediate salt flow rate, and the core outlet temperature with the reactivity provided by the control rods. In the case 1-B, the coupling of the power with the intermediate salt flow rate and of the inlet core temperature with the reactivity appears to be more favourable. Nonetheless, the diagonal pairing, although not recommended by the RGA analysis, is not affected by the same problem that occurs in the case 1-A.

In order to examine the transient response of the closed loop system, two PI controllers have been integrated in the model of the system, according to the scheme shown in Fig. 4. The problem related to the calibration of the control system has been addressed

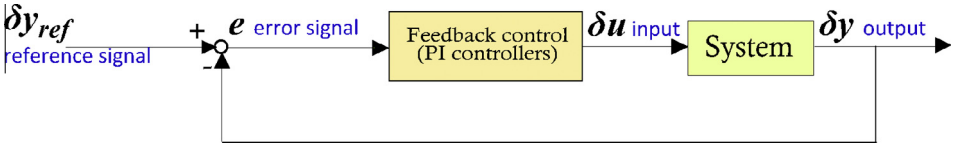

Fig. 4. Schematic representation of the feedback scheme of control adopted in the present work (since we are dealing with a MIMO system, all the indicated variables are intended as vectors). The input and the output of the system represent the control/manipulated variables and the controlled variables, respectively.

providing an estimation of the PI parameters, based on the analysis of the transfer function of each control loop in such a way to assure the effectiveness of the closed loop system in the range of low frequencies while guaranteeing fair stability margins (Åström and Hägglund, 1995). The transient behaviour of the closed loop system is shown in Fig. 5[3], which refers to an 80% power reduction with respect to its nominal value that occurs in three ramps with the duration of 1 min each[4]. During the transient, the core outlet temperature is kept fixed at the nominal value. Finally, the original power level is restored with a slower control action (the duration of the power reference signal rise being of 25 min).

When the core outlet temperature is fixed to its nominal value, the decrease of the power causes an increase of the core average temperature. The temperature feedback provides negative reactivity that must be counterbalanced by the action of the control rods in order to reach a new steady state characterised by a lower power and higher temperatures. As soon as the reduction of the power is required, the coolant flow rate is reduced by the controller. This leads to a decrease of the overall heat transfer coefficient between the primary and the intermediate circuit and the fuel enters the reactor core at a higher temperature. Negative reactivity is provided by the temperature feedback decreasing the power. With the reduction of the power the core outlet temperature tends to decrease, thus positive reactivity is introduced by the control rods to counterbalance the effect of the temperature feedback, allowing the core outlet temperature to remain to its set-point. About 175 pcm are necessary to reduce the power to 20% of the nominal value, without changing the core outlet temperature (Fig. 5b[5]). This reactivity is approximately equal to the effective fraction of delayed neutrons for circulating fuel (170 pcm – computed according to the procedure adopted in (Guerrieri et. al, 2012)).

Fig. 6 shows the response of the system when the controlled variables are the power and the core inlet temperature (case 1-B), for the same power reference signal used in the case 1-A. If the reduction of the power is required while maintaining the core inlet temperature to its set-point, negative reactivity must be inserted by the control rods. The obtained results can be explained as follows. As soon as the power reference signal decreases, the flow rate in the intermediate circuit is reduced by the controller. The temperature at the inlet of the core tends to increase, as explained above, and its error signal causes the insertion of negative reactivity by the control rods. A new steady state is reached when the temperature feedback compensates the external-provided reactivity. The overall effect is the simultaneous reduction of the power and of the average temperature in the core, allowing the core inlet temperature to remain to its nominal value. As in the previous case, the controlled variables exhibit a good behaviour and the relative errors remain below few percents.

[3] In Fig. 5a (and in the subsequent Figs. 6a, 7a, 8a, 9a, 10a and 11a as well), the flow rate variation is normalized with respect to the nominal value reported in Table 1.

[4] This reference signal has been chosen as an example of a fast control action in order to test the performances of the implemented control scheme.

[5] In Fig. 5b (and in the subsequent Figs. 6b and 8b as well), the reactivity variation is normalized with respect to the effective fraction of delayed neutrons for static fuel (318 pcm – see Table 1), whereas 50 °C is used for the normalization of the temperature variations.

Table 5
Case 1-A: RGA of the system with two controlled variables (thermal power and core outlet temperature) and two control variables (control rod-provided reactivity and coolant flow rate).

Case 1-A		
	ρ_{cr}	Γ_2
P	−0.24	**1.24**
$T_f^{c\ out}$	**1.24**	-0.24

Bold values highlight the elements in the RGA matrices that correspond to the chosen input/output pairs.

A third case is of interest in the frame of the present work. It is characterised by the use of only one manipulated variable (i.e., the flow rate in the intermediate circuit) to control the thermal power. Since no reactivity is inserted by the control rods, the system operates with a constant core average temperature, and its transient behaviour is driven by the temperature feedback. In Fig. 7, the results of the simulation are shown for the same power reference signal adopted in the previous cases. As can be observed, even assuming that only the coolant salt flow rate is available as control variable, an effective regulation system for the thermal power can be set up adopting a constant core-average-temperature control strategy.

4.2. Reactivity and flow rate in the primary circuit as control variables

In this subsection, the control rod-provided reactivity and the fuel salt flow rate are used as control variables to regulate the thermal power and one temperature in the core. The RGA referring to the case in which the variables to regulate are the power and the core outlet temperature (case 2-A) has been already shown in Table 4 (case iii-A), whereas the RGA in Table 6 refers to the case in which the power and the core inlet temperature are the controlled variables (case 2-B). In both the analysed scenarios, the RGA analysis suggests to choose the off-diagonal pairing, namely control of the power by varying the primary salt flow rate and of the temperature by means of the reactivity provided by the control rods. This choice is mandatory for the case 2-B, because of the negative elements on the matrix diagonal.

The transient response of the closed loop system has been investigated. Fig. 8 shows the variations of the main quantities of interest for a reduction of the power to 20% of its nominal value, according to the same reference signal previously considered, while keeping fixed the core outlet temperature. As soon as a reduction of the power is required, the primary salt flow rate is reduced by the control system. The core outlet temperature starts to increase due to the reduction of the salt flow rate, while the core inlet temperature decreases because of the longer transit time in the heat exchanger. Without any other control action the overall effect would be an increase of the core average temperature, that would correspond to the insertion of negative reactivity into the system. As soon as the outlet temperature error signal arrives to the PI controller, the control rods provide negative reactivity to the system, to allow a contemporary reduction of the power and of the salt average temperature, while the core outlet temperature remains constant. The total reactivity that must be provided to the

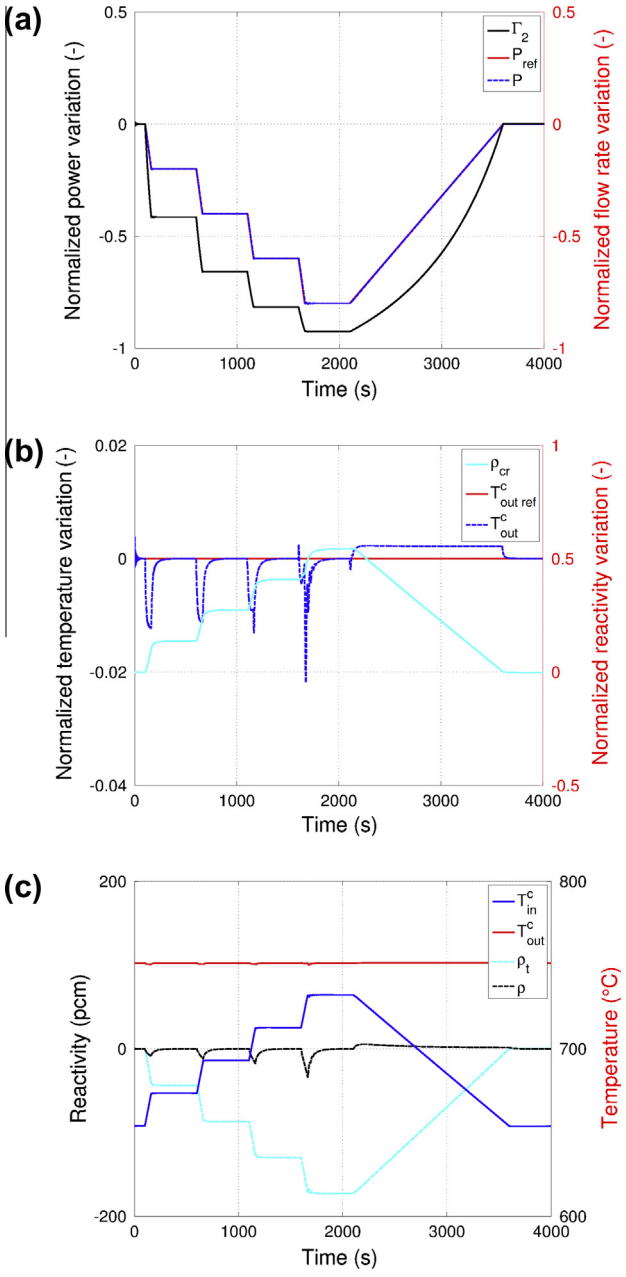

Fig. 5. Transient response of the closed loop system in the case 1-A, in terms of: (a) power variation (reference and actual signals) and coolant flow rate variation (normalised values) – blue and red lines are superimposed; (b) core outlet temperature variation (reference and actual signals) and control rod-provided reactivity (normalised values); (c) inlet and outlet core temperature, reactivity feedback, and total reactivity provided to the system. (For interpretation of the references to colour in this figure legend, the reader is referred to the web version of this article.)

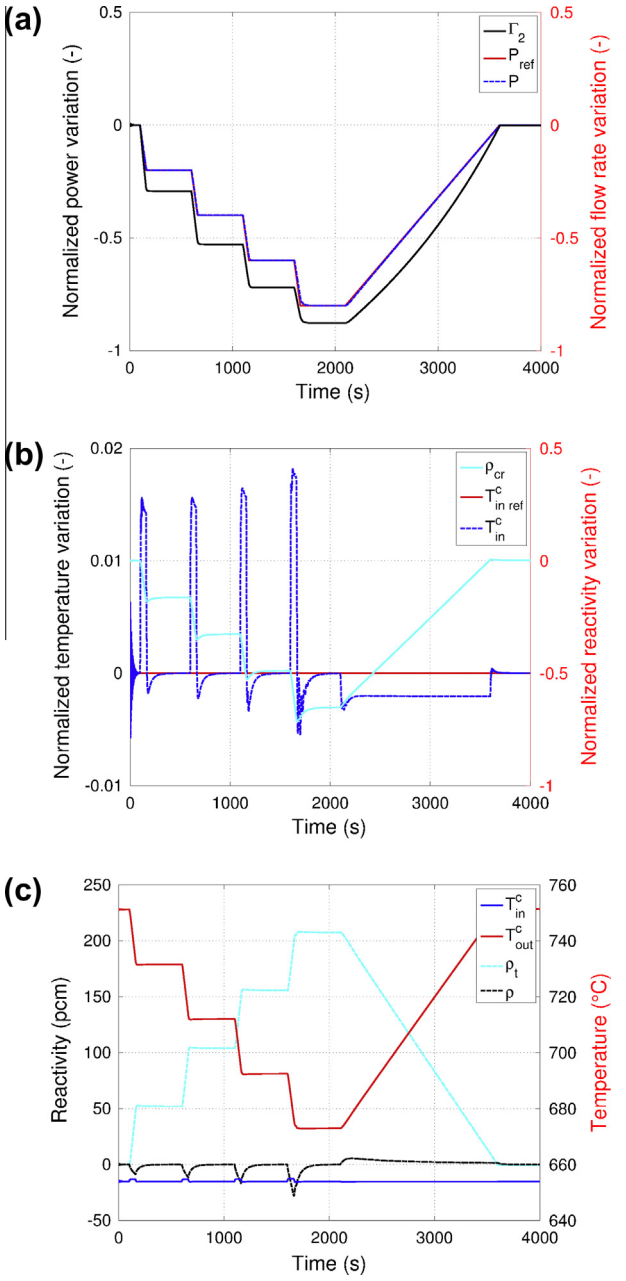

Fig. 6. Transient response of the closed loop system in the case 1-B, in terms of: (a) power variation (reference and actual signals) and coolant flow rate variation (normalised values) – blue and red lines are superimposed; (b) core inlet temperature variation (reference and actual signals) and control rod-provided reactivity (normalised values); (c) inlet and outlet core temperature, reactivity feedback, and total reactivity provided to the system. (For interpretation of the references to colour in this figure legend, the reader is referred to the web version of this article.)

system for a reduction of the power to 20% of its nominal value is equal to 250 pcm (Fig. 8b[5]), which is higher than the effective fraction of delayed neutrons for circulating fuel. It is worth noting that this control scheme is penalising for the management of the temperatures in the core. In fact, because of the reduction of the primary salt flow, the temperature difference between the inlet and the outlet of the core (100 °C in nominal conditions) increases to about 180 °C at 20% of the nominal power and the core inlet temperature approaches the solidification point (~565 °C).

If the controlled variables are the power and the inlet core temperature (case 2-B), the RGA matrix has negative diagonal elements (Table 6). The corresponding pairing is therefore not recommended. This result can be explained as follows. Consider the dynamic behaviour of the system without any control action. A reduction of the primary salt flow rate would cause the decrease of the power, due to the temperature feedback. The average core temperature, in fact, would increase because of the less effective cooling of the core. In the heat exchanger, a lower mass of salt would be cooled down to a temperature lower than the steady state value, and the inlet core temperature would decrease. On the contrary, if the power is kept constant by a control action on the reactivity, the heat up of the salt in the core will be higher and the core inlet temperature, after an initial decrease, will increase. Due to this different behaviour of the system with or

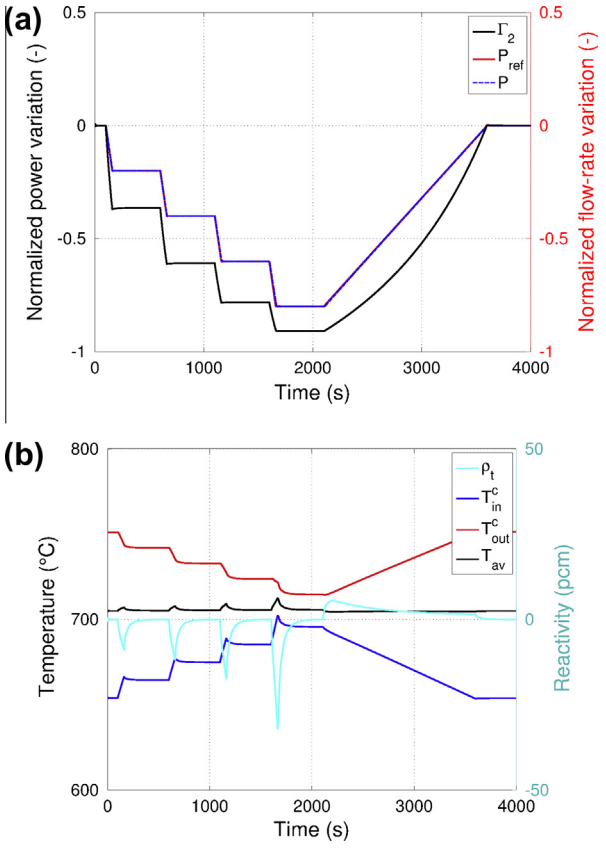

Fig. 7. Transient response of the closed loop system, in terms of: (a) power variation (reference and actual signals) and coolant flow rate variation (normalised values) – blue and red lines are superimposed; (b) inlet, average and outlet core temperature, and reactivity feedback. (For interpretation of the references to colour in this figure legend, the reader is referred to the web version of this article.)

Table 6
Case 2-B: RGA of the system with two controlled variables (thermal power and core inlet temperature) and two control variables (control rod-provided reactivity and flow rate in the primary circuit).

Case 2-B		
	ρ_{cr}	Γ_1
P	−1.21	**2.21**
$T_f^{c\ in}$	**2.21**	−1.21

Bold values highlight the elements in the RGA matrices that correspond to the chosen input/output pairs.

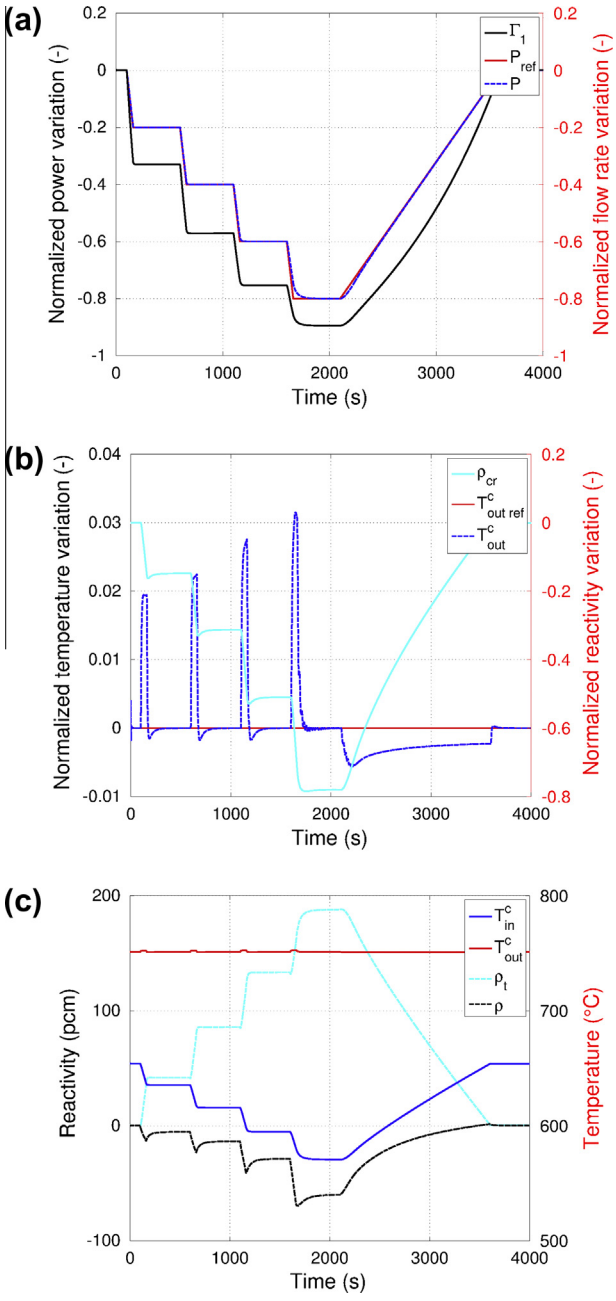

Fig. 8. Transient response of the closed loop system in the case 2-A, in terms of: (a) power variation (reference and actual signals) and fuel salt flow rate variation (normalised values) – blue and red lines are superimposed; (b) core outlet temperature variation (reference and actual signals) and control rod-provided reactivity (normalised values); (c) inlet and outlet core temperature, reactivity feedback, and total reactivity provided to the system. (For interpretation of the references to colour in this figure legend, the reader is referred to the web version of this article.)

without the control action on the power, the only feasible choice is to pair the power with the primary salt flow rate and the core inlet temperature with the reactivity. In this case, the dynamic analysis pointed out a problem of this control scheme. In particular, it was observed that the control of the system becomes very difficult at low power (the results are not shown here for brevity). The cause was identified in the increase of the time delay between the control action (reactivity insertion) and the variation of the controlled variable (core inlet temperature), that occurs when the system operates at low power, due to the reduction of the flow rate in the primary circuit. As long as the error signal on the core inlet temperature is different from zero, the control system inserts positive reactivity in the system. This obstructs the decrease of the power, and the other control loop (featuring the power and the flow rate in the primary circuit) compensates reducing the primary salt flow rate further. As a result, the gains of the PI controllers must be notably reduced to avoid instability of the closed loop system, thus making difficult the effective regulation of the system.

Fig. 9 shows the transient behaviour of the system for the same power reference signal, but using a control strategy with a constant average core temperature. The flow rate in the primary circuit is used to regulate the power and no other control variable is required. Also in this case the reduction of the primary salt flow rate causes a notable increase of the temperature increase between the inlet and the outlet of the core, at low power.

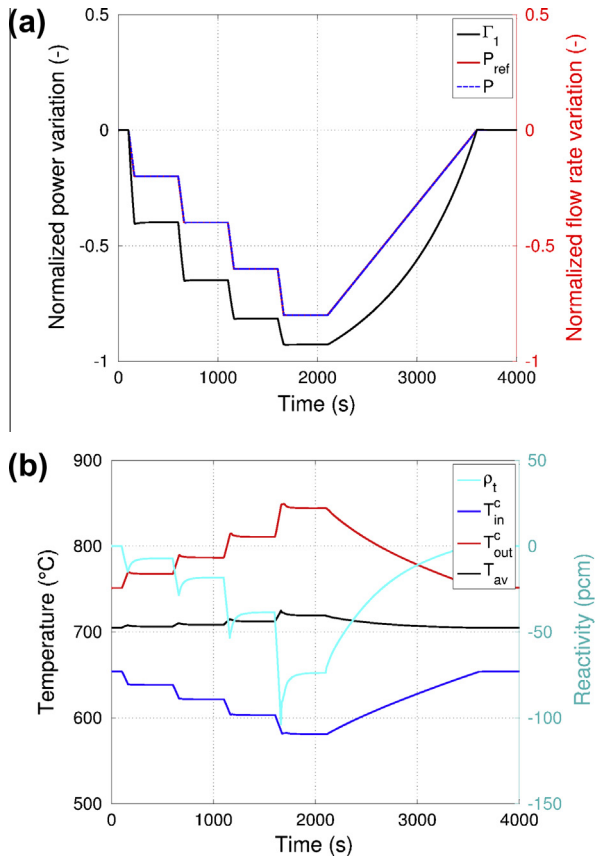

Fig. 9. Transient response of the closed loop system, in terms of: (a) power variation (reference and actual signals) and fuel salt flow rate variation (normalised values) – blue and red lines are superimposed; (b) inlet, average and outlet core temperature, and reactivity feedback. (For interpretation of the references to colour in this figure legend, the reader is referred to the web version of this article.)

Table 7
Case 3-A: RGA of the system with two controlled variables (thermal power and core outlet temperature) and two control variables (flow rates in the primary and intermediate circuits). Case 3-B: RGA of the system with two controlled variables (thermal power and core inlet temperature) and two control variables (flow rates in the primary and intermediate circuits).

Case 3-A			Case 3-B		
	Γ_1	Γ_2		Γ_1	Γ_2
P	0.36	**0.64**	P	0.40	**0.60**
$T_f^{c\ out}$	**0.64**	0.36	$T_f^{c\ in}$	**0.60**	0.40

Bold values highlight the elements in the RGA matrices that correspond to the chosen input/output pairs.

4.3. Flow rates in the primary and intermediate circuits as control variables

The RGA referring to the use of the flow rates in the primary and intermediate circuits to regulate the power and the inlet/outlet core temperature is shown in Table 7. The results are similar for the two analysed cases, and indicate that the off-diagonal pairing must be preferred in order to guarantee a better decoupling of the two control loops used in the decentralized scheme of control.

The dynamic behaviour of the system for the same transient analysed in the previous subsections is shown in Figs. 10 and 11, for the control schemes 3-A and 3-B, respectively.

Fig. 10 shows the transient behaviour of the system, when the power and the outlet core temperature are controlled by means of the coolant salt and fuel salt flow rates, respectively. In order

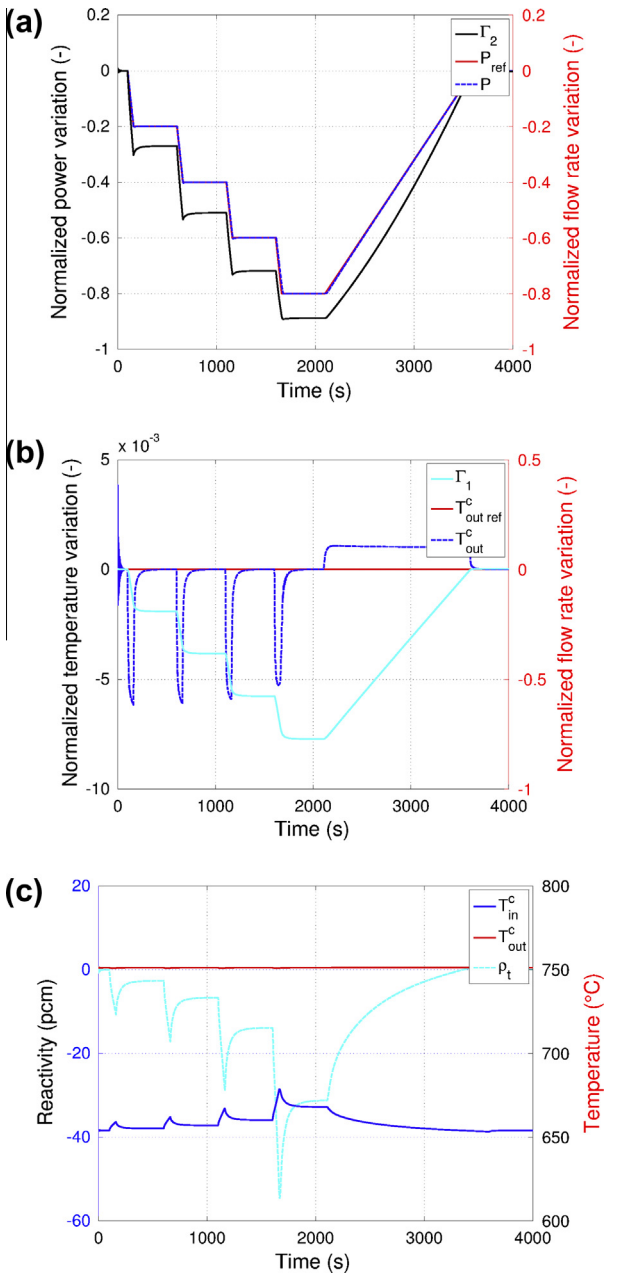

Fig. 10. Transient response of the closed loop system in the case 3-A, in terms of: (a) power variation (reference and actual signals) and coolant flow rate variation (normalised values) – blue and red lines are superimposed; (b) core outlet temperature variation (reference and actual signals) and fuel salt flow rate variation (normalised values); (c) inlet and outlet core temperature, and reactivity feedback. (For interpretation of the references to colour in this figure legend, the reader is referred to the web version of this article.)

to reduce the power according to the reference signal, the flow rate in the intermediate circuit is reduced by the controller. The reduction of the power transferred out towards the heat exchanger causes the core average temperature to increase, and the reactivity feedback acts reducing the power. As the core outlet temperature starts to decrease, the primary salt flow rate is reduced by the second controller, in order to maintain the outlet temperature set-point. Since no reactivity is inserted by the control rods, at each new steady state the reactivity feedback provided by the increase of the average core temperature compensate for the reduction of the fraction of precursors lost in the out-of-core part of the primary circuit, that changes according to the flow rate of the fuel salt.

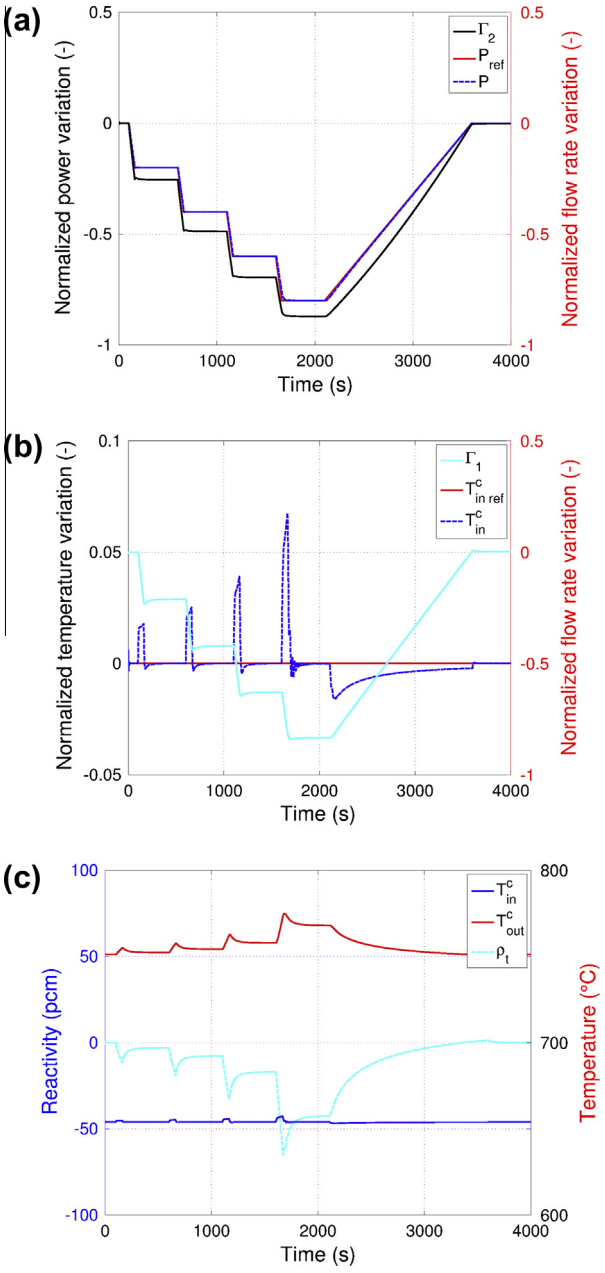

Fig. 11. Transient response of the closed loop system in the case 3-B, in terms of: (a) power variation (reference and actual signals) and coolant flow rate variation (normalised values) – blue and red lines are superimposed; (b) core inlet temperature variation (reference and actual signals) and fuel salt flow rate variation (normalised values); (c) inlet and outlet core temperature, and reactivity feedback. (For interpretation of the references to colour in this figure legend, the reader is referred to the web version of this article.)

Adopting this control strategy, the average core temperature remains almost constant when the power level is varied between 20% and 100% of the nominal value, as well as the temperature increase between the inlet and the outlet of the core.

The general behaviour of the system remains almost the same when the second control scheme (case 3-B) is applied (Fig. 11). Herein, the primary salt flow rate is reduced more than proportionally to the thermal power, and the temperature difference between the inlet and the outlet of the core slightly increases. Also in this case the delay between the control action (variation of the primary salt flow rate) and the response of the controlled variable (i.e., the core inlet temperature) leads to higher errors with respect to the corresponding reference signal, compared with the case 3-A.

5. Conclusions

The present work was aimed at investigating some control issues related to the new MSFR concept, for which the know-how and the experience acquired in the control of conventional nuclear reactors cannot be a priori applied, due to its uncommon design and peculiar dynamic behaviour. Nonetheless, the definition of a control strategy is important for the finalisation and the deployment of this MSR concept. In this work, an objective criterion for the selection of the control loops for a decentralised scheme of control was applied, based on the Relative Gain Array (RGA) analysis, which was proposed as a measure of the interaction that occurs in a MIMO system.

First, a general investigation of the degree of interaction between the input and output variables of the modelled system was performed. Various scenarios were investigated, featured by different set of controlled variables and supposing that, in principle, all the inputs of the system could be used as control variables. It was observed, for example, that a very favourable interaction exists between the reactivity and the temperature in the core (particularly with the core outlet temperature). Therefore, when possible, this pairing should be chosen. Instead, the power should be controlled either by means of the flow rate in the primary circuit or by means of that one in the intermediate circuit.

In the second place, the attention was focused on few scenarios, featuring the regulation of the power and of one temperature in the core. The RGA analysis was used to identify the most favourable I/O pairing, considering three different sets of control variables. The control schemes suggested by the RGA analysis were implemented in the model of the plant, allowing a preliminary evaluation of the transient response of the closed loop system. The dynamic analysis showed that, in the majority of the analysed cases, the implemented control schemes are suitable for the regulation of the system. In these cases, the controlled variables exhibit a good behaviour with relative errors remaining below few percents. A different situation was observed when the control rod-provided reactivity and the fuel flow rate are used as control variables. In particular, in this case, the system control becomes difficult when the reactor operates at low power (if a control scheme of this kind is pursued in the future, further investigation will be needed).

In short, the present work represents a first approach to the MSFR control issues, and provides a preliminary evaluation of possible control options. The analyses highlighted good controllability properties of the MSFR concept. In prospect, the adopted RGA tool is thought to be useful for the finalisation of the control strategy of this reactor, on the basis of more detailed information concerning its design and technological limits.

Acknowledgments

The authors wish to acknowledge the precious collaboration of Prof. Elsa Merle-Lucotte (Laboratoire de Physique Subatomique et de Cosmologie, Grenoble, France) and Dr. Sylvie Delpech (Institut de Physique Nucléaire, Orsay, France), who have kindly provided us with up-to-date information on the MSFR developed in the framework of the Euratom EVOL Project.

References

Åström, K.J., Hägglund, T., 1995. PID Controllers: Theory, Design and Tuning. Instrument Society of America, Research Triangle Park, NC, USA.

Bristol, E.H., 1966. On a new measure of interactions for multivariable process control. IEEE Transactions on Automatic Control 11, 133–134.

Brovchenko, M., Heuer, D., Merle-Lucotte, E., Allibert, M., Capellan, N., Ghetta, V., Laureau, L., 2012. Preliminary safety calculations to improve the design of

Molten Salt Fast Reactor. In: Proc. Int. Conf. PHYSOR 2012, Knoxville, TN, USA, April 15–20, 2012.
Cao, Y., Rossiter, D., 1997. An input pre-screening technique for control structure selection. Computers & Chemical Engineering 21, 563–569.
Chang, J.-W., Yu, C.-C., 1990. The relative gain for non-square multivariable systems. Chemical Engineering Science 45, 1309–1323.
Dittus, F.W., Boelter, L.M.K., 1930. Heat transfer in automobile radiators of the tubular type. University of California Publications in Engineering 2, 443–461.
EVOL Project – Evaluation and Viability of Liquid Fuel Fast Reactor Systems. Available at: <http://www.li2c.upmc.fr/>.
Fiorina, C., Aufiero, M., Cammi, A., Guerrieri, C., Krepel, J., Luzzi, L., Mikityuk, K., Ricotti, M.E., 2012. Analysis of the MSFR core neutronics adopting different neutron-transport models. In: Proc. ICONE20-POWER2012 International Conference, Anaheim, CA, USA, July 30–August 3, 2012.
GIF-IV, Generation IV International Forum, 2002. A Technology Road Map for Generation IV Nuclear Energy Systems. GIF-002–00, US DOE Nuclear Energy Research Advisory Committee and The Generation IV International Forum.
GIF-IV, Generation IV International Forum, 2009. Annual Report. Available at: <http://www.gen-4.org/PDFs/GIF-2009-Annual-Report.pdf>.
Guerrieri, C., Aufiero, M., Cammi, A., Fiorina, C., Luzzi, L., 2012. A preliminary study of the MSFR dynamics. In: Proc. ICONE20-POWER2012 International Conference, Anaheim, CA, USA, July 30–August 3, 2012.
Guerrieri, C., Cammi, A., Luzzi, L., 2013. An approach to MSR dynamics and stability analysis. Progress in Nuclear Energy 67, 56–73.
Hetrick, D.L., 1993. Dynamics of Nuclear Reactors. American Nuclear Society, La Grange Park, IL, USA.
MacPherson, H.G., 1985. The molten salt reactor adventure. Nuclear Science and Engineering 90, 374–380.
Merle-Lucotte, E., Heuer, D., Allibert, M., Brovchenko, M., Capellan, N., Ghetta, V., 2011. Launching the thorium fuel cycle with the Molten Salt Fast Reactor. In: Proc. Int. Conf. ICAPP 2011, Nice, France, May 2–5, 2011.
Rimpault, G., Plisson, D., Tommasi, J., Jacqmin, R., Rieunier, J., Verrier, D., Biron, D., 2002. The ERANOS code and data system for fast reactor neurtonic analyses. In: Proc. Int. Conf. PHYSOR 2002, Seoul, Korea, 7–10 October, 2002.
Simulink®, 2012. Getting Started Guide. The MathWorks, Inc., Natik, MA, USA.
Skogestad, S., Postlethwaite, I., 2001. Multivariable Feedback Control: Analysis and Design. John Wiley & Sons, New York, USA.
Waltar, A.E., Todd, D.R., Tsvetkov, P.V., 2012. Fast Spectrum Reactors. Springer, New York, USA.